ergy minimum for the folded state in Fig. 3A is significantly broader than that in Fig. 3B: The width of this well supplies direct evidence that the nominally folded state for this hairpin actually consists of an ensemble of states with up to ~4 bp unzipped. A similar situation is seen in Fig. 3D, although the slightly steeper well suggests that the fully folded state plays a more dominant role in this mixed ensemble than it does in Fig. 3A. The energy barriers in Figs. 3A and D are clearly different: The barrier in Fig. 3D is wider than in Fig. 3A, indicating a TS that is less well-defined and therefore more susceptible to experimental perturbation, e.g., by mutagenesis or solvent condition changes.

To explore the validity of these measurements, we compared the experimental landscapes with predictions of the model (Fig. 3). We found excellent agreement across the entire landscape for all hairpins studied (within $<1\ k_BT$), with two exceptions. At the lowest extensions, corresponding to regions deconvolved from physical compressions of the double helix (which can arise from thermal fluctuations), as well as elongations, the experimental potential is systematically less stiff than the model. This discrepancy may be attributable to an inaccurate description of the confining potential, somewhat arbitrarily taken to be a Morse potential (*22*). In addition, the barrier for exiting the unfolded state in Fig. 3B rises to the TS more slowly than predicted, lagging by up to $3\ k_BT$ at the point of greatest discrepancy. We speculate that this deviation may result from the large number of base pairs that must be formed to reach the TS from the unfolded state, which allows more opportunities for abortive refolding attempts involving misfolded base pairs. In principle, the sequence for this particular hairpin allows for a number of misfolded states containing short, 2- to 3-bp helices. Any such misfolding, neglected in the model, would tend to increase the probability of extensions near the unfolded state, exactly as observed.

The deconvolution approach described here has known limitations. To obtain adequate statistics, folding must occur sufficiently frequently that large numbers of transitions can be recorded. In the present case, this places a practical limit on the folding rate of $\sim 0.1\ s^{-1}$, which is faster than some slow folding transitions found in proteins or ribozymes. The numerical stability of any deconvolution process depends on the quality of the input data (both for the record being analyzed and the PSF used). In practice, only a limited range of frequency information can be recovered by deconvolution, which restricts the resolution of the reconstructed landscape, particularly at the shortest length scales (*23*). Moreover, experimental noise may become amplified by deconvolution, which produces artifactual features that further complicate determinations of short-scale behavior (*21*) The challenges posed by deconvolution, however, may be mitigated by increasing the stiffness of the experimental system, which reduces the smoothing of trajectories (*24*). Improvements may be achieved by increasing the stiffness of the handles (e.g., by making them shorter or from materials other than dsDNA). Application of the approach described here to peptides or more complex nucleic acid sequences may supply further insights into how energy landscapes guide the folding process.

References and Notes

1. A. Fersht, *Structure and Mechanism in Protein Science* (Freeman, New York, 1999).
2. D. Petrey, B. Honig, *Mol. Cell* **20**, 811 (2005).
3. P. Bradley, K. M. S. Misura, D. Baker, *Science* **309**, 1868 (2005).
4. C. M. Dobson, *Nature* **426**, 884 (2003).
5. J. N. Onuchic, P. G. Wolynes, *Curr. Opin. Struct. Biol.* **14**, 70 (2004).
6. V. Daggett, A. R. Fersht, *Trends Biochem. Sci.* **28**, 18 (2003).
7. P. S. Kim, R. L. Baldwin, *Annu. Rev. Biochem.* **59**, 631 (1990).
8. C. Hyeon, D. Thirumalai, *Proc. Natl. Acad. Sci. U.S.A.* **100**, 10249 (2003).
9. J. Buchner, T. Kiefhaber, Eds., *Protein Folding Handbook* (Wiley-VCH, Weinheim, Germany, 2005).
10. J. Liphardt, B. Onoa, S. B. Smith, I. Tinoco Jr., C. Bustamante, *Science* **292**, 733 (2001).
11. B. Onoa *et al.*, *Science* **299**, 1892 (2003).
12. P. T. X. Li, D. Collin, S. B. Smith, C. Bustamante, I. Tinoco Jr., *Biophys. J.* **90**, 250 (2006).
13. M. T. Woodside *et al.*, *Proc. Natl. Acad. Sci. U.S.A.* **103**, 6190 (2006).
14. W. J. Greenleaf, M. T. Woodside, E. A. Abbondanzieri, S. M. Block, *Phys. Rev. Lett.* **95**, 208102 (2005).
15. Materials and methods are available as supporting material on *Science* Online.
16. G. I. Bell, *Science* **200**, 618 (1978).
17. Because all lifetimes were measured at $F_{1/2}$, the folded and unfolded states were nearly isoenergetic for every hairpin, and Hammond behavior was neither expected nor observed.
18. J. M. Fernandez, S. Chu, A. F. Oberhauser, *Science* **292**, 653 (2001).
19. H. A. Kramers, *Physics* **7**, 284 (1940).
20. Experimentally determined probability densities have been used to measure the energy landscape for a micron-scale bead hopping between adjacent optical traps (*25*), to probe the elasticity of kinesin molecules (*26*), and to support the existence of otherwise hidden intermediate states based on thermal fluctuations (*27*), but not to measure the energy landscape for a molecular transition.
21. P. A. Jansson, Ed., *Deconvolution of Images and Spectra* (Academic Press, New York, ed. 2, 1997).
22. A likely explanation for the weak confining potential observed experimentally is that the hairpin can rotate, effectively producing extensions lower than the folded state as the handles move past one another, driven by thermal fluctuations.
23. In practice, we found a resolution limit of ~2 nm, which includes the effects of instrumental drift.
24. We measured the probabilities and free energy in an unclamped configuration (data in Fig. 3, A to C) because passive force-clamping reduces the system stiffness (*14*).
25. L. I. McCann, M. Dykman, B. Golding, *Nature* **402**, 785 (1999).
26. S. Jeney, E. H. K. Stelzer, H Grubmüller, E.-F. Florin, *Chem Phys Chem* **5**, 1150 (2005).
27. K. A. Walther, J. Brujić, H. Li, J. M. Fernandez, *Biophys. J.* **90**, 3806 (2006).

28. We thank members of the Block lab and the Ribozyme Folding Project for helpful discussions and manuscript comments. Supported by NIH PO1-GM066275.

Supporting Online Material

www.sciencemag.org/cgi/content/full/314/5801/1001/DC1
Materials and Methods
Figs. S1 and S2
Tables S1 and S2
References

8 August 2006; accepted 29 September 2006
10.1126/science.1133601

Ion Selectivity in a Semisynthetic K^+ Channel Locked in the Conductive Conformation

Francis I. Valiyaveetil,* Manuel Leonetti, Tom W. Muir,† Roderick MacKinnon†

Potassium channels are K^+-selective protein pores in cell membrane. The selectivity filter is the functional unit that allows K^+ channels to distinguish potassium (K^+) and sodium (Na^+) ions. The filter's structure depends on whether K^+ or Na^+ ions are bound inside it. We synthesized a K^+ channel containing the D-enantiomer of alanine in place of a conserved glycine and found by x-ray crystallography that its filter maintains the K^+ (conductive) structure in the presence of Na^+ and very low concentrations of K^+. This channel conducts Na^+ in the absence of K^+ but not in the presence of K^+. These findings demonstrate that the ability of the channel to adapt its structure differently to K^+ and Na^+ is a fundamental aspect of ion selectivity, as is the ability of multiple K^+ ions to compete effectively with Na^+ for the conductive filter.

Potassium channels are exquisitely selective for K^+ over Na^+, even though Na^+ (Pauling ionic radius 0.95 Å) is smaller than K^+ (Pauling ionic radius 1.33 Å) (*1*). The selection of K^+ and rejection of Na^+ occurs in a segment of the ion conduction pathway called the K^+ selectivity filter (*2*). The filter binds two fully dehydrated K^+ ions by providing protein oxygen atoms that offset the energy cost of ion dehydration (*3*, *4*). Conduction occurs when a third K^+ ion enters and a resident K^+ ion exits in a concerted manner. The Na^+ ion is virtually excluded from conducting through the selectivity filter (*5*, *6*).

The K^+ selectivity filter adopts a fundamentally different atomic structure depending on whether K^+ or Na^+ is present in the solution in

which the channel is crystallized (*3*, *4*). In solutions containing K^+ (≥20 mM), the KcsA K^+ channel selectivity filter exhibits four K^+ binding sites designated sites 1 through 4 (Fig. 1A), whereas in solutions containing Na^+ (3 mM K^+, 150 mM Na^+) the filter adopts a "collapsed" conformation that no longer contains native binding sites at sites 2 and 3 (Fig. 1B). The K^+ structure is referred to as "conductive" because the queue of K^+ ions within the filter connects the intracellular and extracellular solutions. The Na^+ structure is referred to as "nonconductive" because the filter is pinched shut in the middle. The conformational changes that occur in going from the nonconductive to the conductive structure involve protein atoms that directly coordinate K^+ ions as well as atoms buried within the protein core up to a distance of 15 Å away from the ion pathway (Fig. 1, C and D) (*4*).

The binding of K^+ ions to the filter drives the conformational change from nonconductive to conductive: In crystal structures, the transition occurs between 3 mM and 20 mM K^+ (while maintaining ionic strength constant with Na^+) (*3*). This means that Na^+ (or the absence of K^+) favors the nonconductive conformation and K^+ stabilizes the conductive conformation. At an intuitive level, this is clearly a beneficial property of a molecular device whose function is to conduct K^+ and prevent Na^+ conduction. At a more detailed analytic level, the differential response of the filter's structure to K^+ and Na^+ implies two important features of K^+ selectivity. First, ion selectivity is a property of the protein structure not just locally (at the ion-binding sites) but also globally, because the conformational changes associated with the binding of K^+ ions extend far from the binding sites. Second, ion selectivity may be inextricably linked to the multi-ion nature of the K^+ selectivity filter, because the filter must contain two K^+ ions to achieve its conductive conformation.

One way to investigate the importance of the K^+-induced conformational change is to interfere with it and see how selectivity is affected. The conformational change from conductive to nonconductive involves a rotation of the main chain at Gly^{77} that brings about occlusion of ion site 2 by the α-CH_2 of the glycine (Fig. 1, A and B). The role of Gly^{77} as a surrogate D–amino acid has been demonstrated through synthesis of a functional KcsA K^+ channel with a D-alanine at position 77 ($KcsA^{D\text{-}Ala77}$) (*7*). We have now determined the crystal structure of this channel

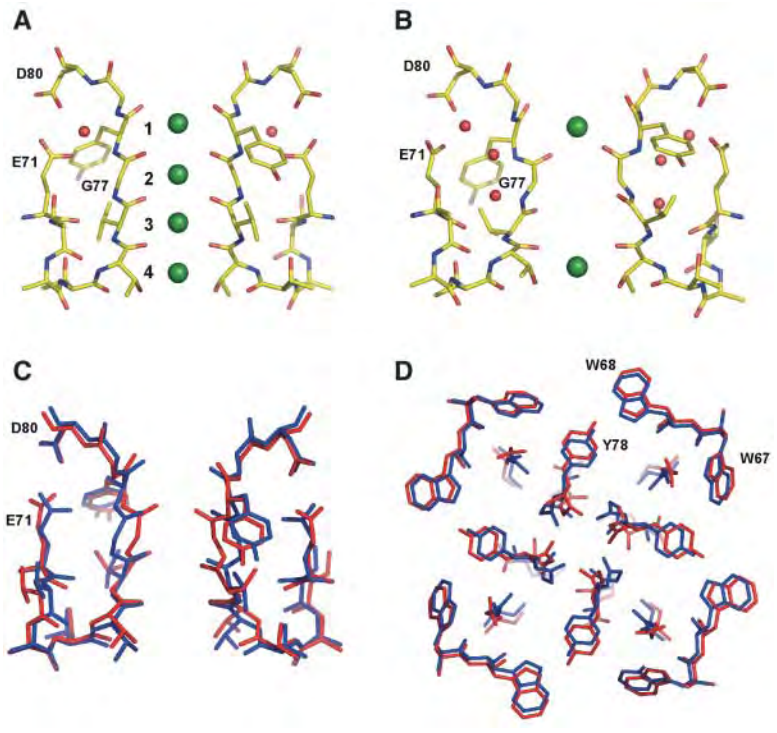

Fig. 1. Dependence of the conformation of the selectivity filter of K^+ channels on K^+ concentration. (**A**) Close-up view of the selectivity filter of wild-type KcsA channel in the presence of high K^+ concentrations [K^+]. Two of the diagonally opposite subunits are shown in stick representation. K^+ ions are depicted as green spheres and water molecules as red spheres. The K^+ binding sites in the selectivity filter are labeled. (**B**) The structure of the selectivity filter in low [K^+], represented as in (A). (**C** and **D**) Superposition of the selectivity filter of wild-type KcsA in the presence of high [K^+] (blue) and low [K^+] (red). (C) shows a side view; (D) depicts a top view extending ~15 Å out from the center of the filter. Aromatic residues that undergo conformation changes are indicated.

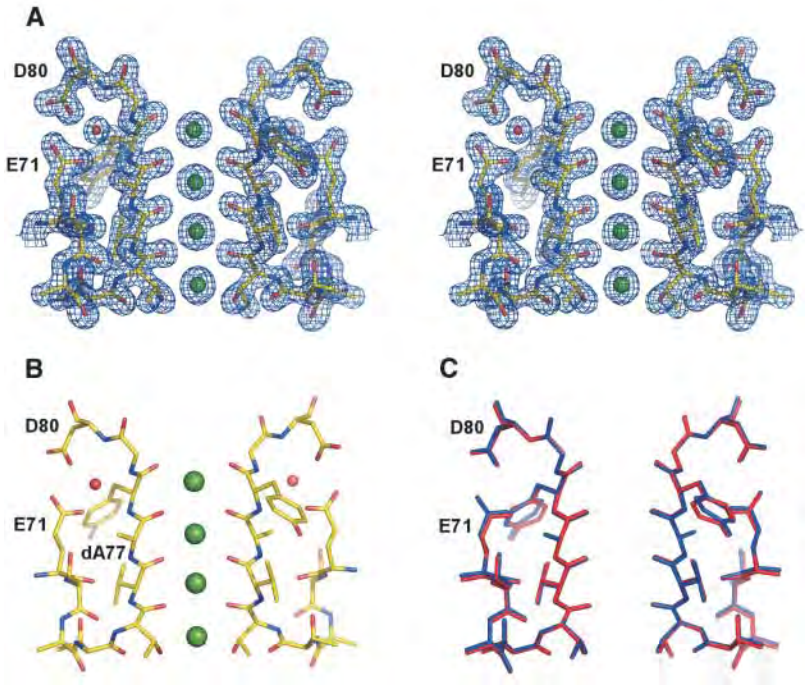

Fig. 2. Structure of the selectivity filter of $KcsA^{D\text{-}Ala77}$ in the presence of high [K^+]. (**A**) Stereo view of the electron density of the selectivity filter of $KcsA^{D\text{-}Ala77}$. The $2F_{obs} - F_{calc}$ electron density map contoured at 2.0σ for the diagonally opposite subunits is shown. (**B**) Structure of the selectivity filter of $KcsA^{D\text{-}Ala77}$ in high [K^+] represented as in Fig. 1. (**C**) Superposition of the selectivity filter of $KcsA^{D\text{-}Ala77}$ (blue) and the wild-type KcsA channel (red) in the presence of high [K^+].

Laboratories of Molecular Neurobiology and Biophysics and Synthetic Protein Chemistry, Rockefeller University and Howard Hughes Medical Institute, 1230 York Avenue, New York, NY 10021, USA, and Department of Biology, Ecole Normale Superieure, 46 rue d'Ulm, 75005 Paris, France.

*Present address: Department of Physiology and Pharmacology, Oregon Health Sciences University, 3181 SW Sam Jackson Park Road, Mail Code L334, Portland, OR 97239, USA.

†To whom correspondence should be addressed. E-mail: mackinn@rockefeller.edu (R.M.), muirt@rockefeller.edu (T.W.M.)

with data to 1.7 Å Bragg spacings in a solution containing 150 mM K^+ (Fig. 2A). Aside from the additional methyl group from D-alanine, the structure of $KcsA^{D\text{-}Ala77}$ is essentially identical to the wild-type conductive structure (Fig. 2, B and C), with a root-mean-square deviation of 0.16 Å for all non-hydrogen atoms from positions Glu^{71} to Asp^{80}.

The important aspect of $KcsA^{D\text{-}Ala77}$ for the present study is depicted in Fig. 3, A and B. Shown is the predicted structure of $KcsA^{D\text{-}Ala77}$ if it were to adopt the nonconductive conformation similar to the wild-type KcsA channel (Fig. 3B). The four methyl groups of the D-alanine (one from each subunit) should prevent this conformation because they clash with each other. Thus, in principle, $KcsA^{D\text{-}Ala77}$ should be forced to remain in the conductive conformation through destabilization of the nonconductive conformation. To test whether this is indeed the case, we determined the structure of $KcsA^{D\text{-}Ala77}$ in the presence of 149 mM Na^+ + 1 mM K^+ with data to 2.4 Å Bragg spacings. At this low K^+ ion concentration, the wild-type channel adopts the nonconductive conformation but $KcsA^{D\text{-}Ala77}$ clearly adopts the conductive conformation (Fig. 3, C and D). Electron density for ions in the filter suggests reduced occupancy. If we assume that the ions are K^+, then the sum of occupancies for all four sites is ~1.1 compared to 1.8 for $KcsA^{D\text{-}Ala77}$ in 150 mM K^+ and 2.1 for wild-type KcsA in 150 mM K^+ (*3*). An alternative explanation for the reduced electron density in $KcsA^{D\text{-}Ala77}$ at 149 mM Na^+ + 1 mM K^+ is that Na^+ may begin to replace K^+. The most important point, however, is that the protein structure of $KcsA^{D\text{-}Ala77}$ is essentially the same in 1 mM and 150 mM K^+ (Fig. 3E), and both of these structures are similar to the conductive structure of the wild-type channel (Fig. 2C). Therefore, the $KcsA^{D\text{-}Ala77}$ channel appears to be captured in the conductive conformation at low concentrations of K^+.

To test the effect of this phenomenon on ion selectivity, we reconstituted the $KcsA^{D\text{-}Ala77}$ channel into planar lipid membranes and studied its properties in various mixtures of K^+ and Na^+ (Fig. 4). With 150 mM K^+ in the internal solution and 20 mM K^+ + 130 mM Na^+ in the external solution, the current reverses very near the calculated Nernst potential for the K^+ gradient (–52 mV), which means that the channel selects K^+ under these conditions (Fig. 4A). With 150 mM Na^+ in the internal solution and 150 mM K^+ in the external solution, inward current is observed at all voltages (Fig. 4B). Alternatively, when the K^+ solution is placed on the inner side of the membrane and Na^+ on the external side, only outward current (or zero current) is observed at all voltages (Fig. 4C). These results indicate that the $KcsA^{D\text{-}Ala77}$ channel conducts only K^+ in mixtures of Na^+ and K^+.

Wild-type–like selectivity in the presence of high K^+ concentrations is not surprising because the structure of the $KcsA^{D\text{-}Ala77}$ channel is essentially identical to that of the wild-type channel at high K^+ concentrations. Structural differences between these channels only occur in solutions with low K^+ concentrations, in which the wild-type channel adopts the nonconductive conformation and the $KcsA^{D\text{-}Ala77}$ channel remains in the conductive conformation. In the absence of K^+ and presence of 150 mM Na^+ on both sides of the membrane, the $KcsA^{D\text{-}Ala77}$ channel conducts Na^+ (Fig. 4D). The Na^+ current is definitely mediated by the K^+ channel because it is completely blocked by the specific K^+ channel inhibitor agitoxin2 ($AgTx_2$) (*8*). The wild-type KcsA K^+ channel does not conduct Na^+ in the absence of K^+ (Fig. 4E). In this experiment the presence of channels in the membrane is first documented by having K^+ on one side of the membrane, and then K^+ is replaced with Na^+ with the use of a perfusion apparatus.

To summarize the data, the wild-type KcsA K^+ channel prevents Na^+ from conducting through its filter, whether or not K^+ is present in solution. The $KcsA^{D\text{-}Ala77}$ channel prevents Na^+ conduction as long as K^+ is present but conducts Na^+ if K^+ is absent. These channels differ in that $KcsA^{D\text{-}Ala77}$ fails to enter the nonconductive conformation when the K^+ concentration is lowered. This result implies that a conductive filter structure in the absence of K^+ will allow Na^+ to conduct. From this we infer that K^+ channels normally prevent Na^+ conduction in solutions with very low K^+ not because Na^+ is unable to diffuse across the conductive filter, but because Na^+ (or the absence of K^+) favors the nonconductive conformation.

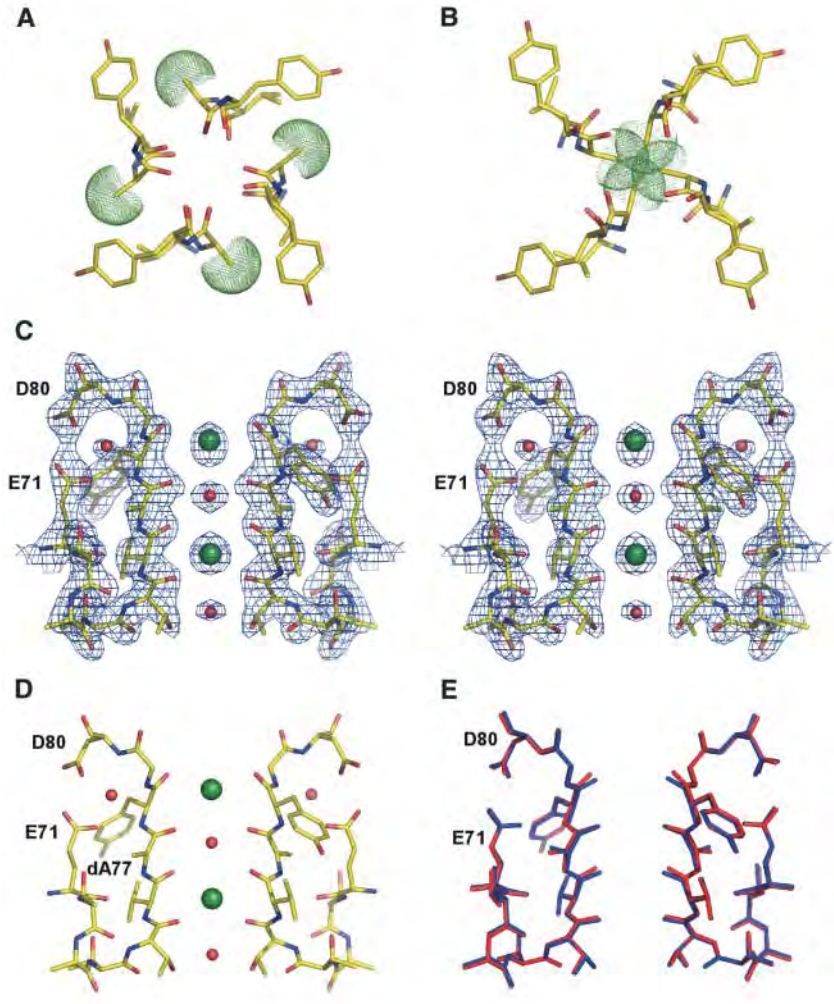

Fig. 3. Structure of the selectivity filter of $KcsA^{D\text{-}Ala77}$ in the presence of low $[K^+]$. (**A**) Top view of the structure of the selectivity filter of $KcsA^{D\text{-}Ala77}$ in high $[K^+]$. The methyl side chain of the D-Ala residue in each of the four subunits is shown in van der Waals (VDW) sphere representation. (**B**) A hypothetical structure of $KcsA^{D\text{-}Ala77}$ in the low $[K^+]$ collapsed state. The methyl side chain of the D-Ala residue is again shown in VDW sphere representation. (**C**) Stereo view of the electron density of the selectivity filter of $KcsA^{D\text{-}Ala77}$ in the presence of low $[K^+]$. The $2F_{obs} - F_{calc}$ electron density map contoured at 2.0σ for the diagonally opposite subunits is shown. (**D**) The structure of the selectivity filter of $KcsA^{D\text{-}Ala77}$ in low $[K^+]$ represented as in Fig. 1. (**E**) Superposition of the selectivity filter of the $KcsA^{D\text{-}Ala77}$ in high $[K^+]$ (blue) and low $[K^+]$ (red).

The adaptive nature of the filter conformation is not the sole basis of ion selectivity. An additional layer of ion selectivity is revealed by the KcsA$^{D\text{-}Ala77}$ channel, which selectively conducts K^+ in the presence of Na^+ even though its selectivity filter is locked in the conductive conformation. Selectivity in this case can be understood if K^+ successfully competes for the binding sites in the conductive form of the filter. In other words, the two K^+ ions residing in the conductive filter block Na^+ conduction. Because the presence of two K^+ ions is a prerequisite for the formation of the conductive conformation in the wild-type channel, Na^+ ions will be unable to permeate. This explanation is not inconsistent with the conduction of Na^+ through the conductive filter in the absence of K^+ (which is only observable in the KcsA$^{D\text{-}Ala77}$ channel). When Na^+ enters the filter in the absence of competing K^+ ions, we do not know whether Na^+ is partially hydrated or how it interacts with the binding sites.

The above discussion underscores two essential ideas: first, that the ability of the selectivity filter to adapt structurally in an ion-specific manner to K^+ and Na^+ is a fundamental aspect of ion selectivity, and second, that the prevention of Na^+ conduction in solutions containing both K^+ and Na^+ is connected directly to the selective nature of the binding sites in the conductive filter, which binds multiple K^+ preferentially over Na^+ when these two ions compete for the binding sites.

Selective conduction of K^+ over Na^+ ultimately stems from the filter's ability to adopt different structures in response to K^+ and Na^+ as well as from the selective nature of multiple binding sites in the conductive filter, which enable K^+ to compete against Na^+. The ability to adopt a conductive conformation in response to K^+, in which the binding sites are size-matched to K^+, is a property of the protein structure. We predict that attempts to synthesize novel K^+ selectivity filters will be successful only if the structures can capture the correct responsiveness to K^+ versus Na^+ (*9*). Attempts to understand K^+ selectivity through computation must take into account the entire selectivity filter occupied by two K^+ ions, because the experiments here show that an "empty" filter conducts Na^+.

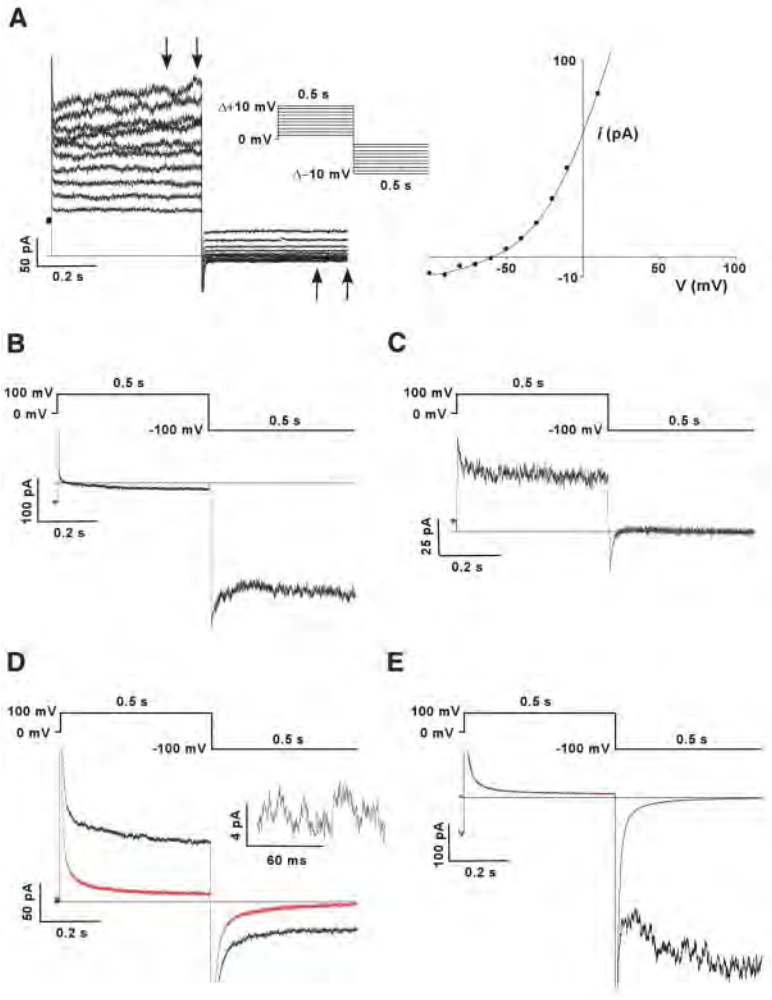

Fig. 4. Electrophysiological characterization of KcsA$^{D\text{-}Ala77}$. (**A**) Determination of ionic selectivity. Macroscopic currents were recorded using 10 mM succinate and 150 mM KCl (pH 4.0) as the internal solution, and 10 mM Hepes, 20 mM KCl, and 130 mM NaCl (pH 7.0) as the external solution. Current values between the time points indicated by arrows were averaged and plotted against the voltage applied for determining the reversal potential (Nernst potential = −52.3 mV). (**B**) Currents for KcsA$^{D\text{-}Ala77}$ were recorded using 10 mM succinate and 150 mM NaCl (pH 4.0) as the internal solution, and 10 mM Hepes and 150 mM KCl (pH 7.0) as the external solution. (**C**) Currents for KcsA$^{D\text{-}Ala77}$ were recorded using 10 mM succinate and 150 mM KCl (pH 4.0) as the internal solution, and 10 mM Hepes and 150 mM NaCl (pH 7.0) as the external solution. For (A) to (C), leak currents were determined by blocking channel currents using 5 μM $AgTx_2$ and were subtracted. (**D**) Currents for KcsA$^{D\text{-}Ala77}$ were recorded using 10 mM succinate and 150 mM NaCl (pH 4.0) as the internal solution, and 10 mM Hepes and 150 mM NaCl (pH 7.0) as the external solution. The amount of leak current was determined by the addition of 5 μM $AgTx_2$ (red trace). Inset is a magnified view of the current traces showing KcsA$^{D\text{-}Ala77}$ channel activity in the presence of Na^+. (**E**) Currents for wild-type KcsA were recorded using 10 mM succinate and 150 mM NaCl (pH 4.0) as the internal solution, and 10 mM Hepes and 150 mM KCl (pH 7.0) as the external solution (black trace). Also shown is the current after replacement of the external solution with 10 mM Hepes and 150 mM NaCl (pH 7.0) by perfusion (blue trace). The amount of leak current was determined by the addition of 5 μM $AgTx_2$ (broken red trace).

References and Notes

1. B. Hille, *Ionic Channels of Excitable Membranes* (Sinauer Associates, Sunderland, MA, ed. 3, 2001).
2. D. A. Doyle *et al.*, *Science* **280**, 69 (1998).
3. Y. Zhou, R. MacKinnon, *J. Mol. Biol.* **333**, 965 (2003).
4. Y. Zhou, J. H. Morais-Cabral, A. Kaufman, R. MacKinnon, *Nature* **414**, 43 (2001).
5. J. H. Morais-Cabral, Y. Zhou, R. MacKinnon, *Nature* **414**, 37 (2001).
6. M. LeMasurier, L. Heginbotham, C. Miller, *J. Gen. Physiol.* **118**, 303 (2001).
7. F. I. Valiyaveetil, M. Sekedat, R. MacKinnon, T. W. Muir, *Proc. Natl. Acad. Sci. U.S.A.* **101**, 17045 (2004).
8. R. MacKinnon, S. L. Cohen, A. Kuo, A. Lee, B. T. Chait, *Science* **280**, 106 (1998).
9. J. C. Mareque Rivas, H. Schwalbe, S. J. Lippard, *Proc. Natl. Acad. Sci. U.S.A.* **98**, 9478 (2001).

10. We thank S.-Y. Lee for assistance with crystallographic data collection and analysis, and E. Gouaux for providing computer access to F.I.V. Supported by NIH grants EB001991 and GM55843 (T.W.M.) and GM43949 (R.M.). R.M. is an Investigator of the Howard Hughes Medical Institute. The high- and low-K^+ KcsA$^{D\text{-}Ala77}$ structure coordinates and reflection files are deposited in the Protein Data Bank under accession numbers 2IH3 and 2IH1, respectively.

Supporting Online Material

www.sciencemag.org/cgi/content/full/314/5801/1004/DC1
Materials and Methods
Table S1
References

3 August 2006; accepted 10 October 2006
10.1126/science.1133415